FATIGUE DAMAGE EVALUATION IN CERAMIC MATRIX COMPOSITES

Stéphane **Baste**
Université Bordeaux I
Laboratoire de Mécanique Physique, URA C.N.R.S. 867
351 Cours de la Libération 33405 Talence cedex, France

INTRODUCTION

Damage is conventionally defined as the progressive deterioration of materials due to nucleation and growth of microcracks. The purpose of the damage concept [1] is to take into account the microscopic deterioration of the material in its macroscopic constitutive law. In composite materials, the microcracks have a preferential orientation and the damage variable depends on the direction of measurement [2]. Non linear analysis of such materials must consider this anisotropy by introducing a tensorial damage variable in the constitutive equations [3]. The main difficulties when dealing with anisotropic description of damage are to be able to identify the introduced parameters [4].

The feasibility of the ultrasonic evaluation of damage has already been shown [5, 6]. The ultrasonic technique makes it possible to measure the stiffness tensor of an anisotropic material [7, 8]. The use of an immersed ultrasonic device connected to a tensile machine makes it possible to perform the measurements of the nine stiffness coefficients describing completely the elasticity of an orthotropic material during a tensile test [9, 10].

The objective of the present investigation is a full characterization of the anisotropic damage accumulation during fatigue of a ceramic matrix composite. Damage is measured by the variation of the all set of elasticity coefficients during fatigue cycles in order to identify the representative damage parameter and the mechanisms responsible for the degradation and for the failure.

Review of Progress in Quantitative Nondestructive Evaluation, Vol. 14
Edited by D.O. Thompson and D.E. Chimenti, Plenum Press, New York, 1995

FATIGUE DAMAGE MECHANISMS

Ceramic matrix composites exhibit a non-catastrophic failure coupled to a non-linear behavior under tension loading [11]. This behavior is due to various energy dissipating mechanisms such as transverse matrix microcracking, fiber/matrix debonding and/or sliding and fiber pull-out [12]. Whether the failure mechanisms (matrix cracking, which can be intralaminar or interlaminar (delamination), interface failure (fiber-matrix debonding), and fiber fracture, slitting or buckling [13]) in an epoxy matrix composite laminate are well identified, no definitive explanations of the fatigue mechanisms in ceramic matrix composites appear to have been made. However, several authors agree with the fact that the changes caused in the microstructure in the first load cycle are the most substantial and apparently govern the behavior in the following cycle [14, 15]. The Young's modulus in the loading direction was more often than not used to detect the initiation and the growth of the damage modes. The effect of the transverse matrix microcracking on this modulus is significant [16]. This mode usually occurs during the first loading cycle. Since a crack in a brittle solid is, by definition, unstable, all transverse matrix cracking would be complete in the very first load cycles, leaving no cause for further cracking in subsequent cycles. That explain the plateau in change in the Young's modulus.

Longitudinal cracking, dispersed or localized, is a particularity active mode of damage. Unfortunately, degradation by longitudinal micro-cracking affects not the longitudinal Young's modulus [17]. That means that no assessment about this damage mode development can be done by this modulus. A full evaluation cannot be achieved by the classical static technique and it leads to a very limited damage evaluation. Clearly, Young modulus variations are not significant for fatigue. Ultrasonic evaluation techniques make it possible to measure the nine stiffness coefficients describing completely the elasticity of an orthotropic material is required for anisotropic damage evaluation.

MATERIAL AND EXPERIMENTAL PROCEDURE

The material studied is a bi-directional carbon-SiC composite prepared by S.E.P. It is fabricated from 2D fibrous preform built up from multiple layers of Carbon cloths. The SiC matrix was added by a chemical vapor infiltration process. Before infiltration by the matrix, the carbon fibers were coated with a pyrocarbon interphase of mean thickness of about 1 mm to enhance the desired non-catastrophic tensile behavior [18]. These processing steps resulted in a material having a density close to 2, a fiber content of approximately 40 Vol% and a residual porosity inherent to the CVI process in the range 10-15 %.

Tension-tension fatigue tests were performed under load control at a sinusoidal frequency of 1 Hz and a constant stress ratio of 0.1 for maximum stresses of 360 MPa using large flat specimens of 190 mm total length. Fatigue damage accumulation was followed by regularly interposed ultrasonic characterization cycles.

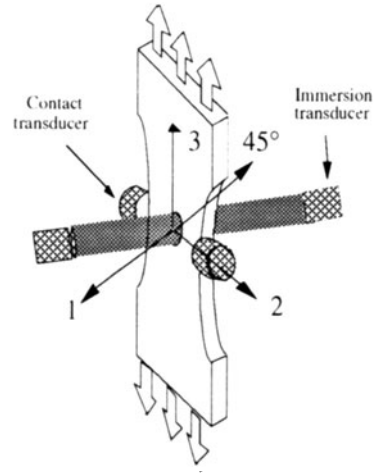

Figure 1. Under load ultrasonic device.

The main principles and methods of the recovery of the elastic constants of anisotropic materials have been thoroughly described elsewhere [7, 8]. Stiffnesses hare recovered as the coefficients of the secular equation [19] from suitable sets of experimental velocities in various directions [20]. This inversion method minimizes, in the least square sense, the shift between the experimental values, and the one calculated from the secular equation for the optimum values of the stiffnesses. For a thin plate sample, the measurements made in the two accessible principal planes lead to the identification of seven coefficients of the stiffness tensor, namely: C_{11}, C_{22}, C_{12}, C_{66} for a propagation in the plane (1, 2) (in axes of Fig. 1), and C_{11}, C_{33}, C_{13}, C_{55} in the plane (1, 3). The two remaining coefficients C_{23} and C_{44} are identified by propagation in the non-principal plane of symmetry (1, 45°) of orthorhombic materials [8]. Axis 45° is defined as the bisecting line of the axes 2 and 3 (see Fig. 1). For tetragonal material, this plane is a plane of symmetry and those two stiffnesses can be not measured independently [21]. The value of C_{44} is measured with contact transducers.

ANISOTROPIC DAMAGE MODEL

The changes in the internal structure occurring in materials under stress affect their physical and mechanical properties. Degradation of one of those properties is an indirect measurement of damage. Changes in the values of the elastic stiffnesses can be taken as a characterization of the state of damage. The elasticity tensor can be written in an additive form [22]:

$$C = C_0 - C_c \ , \qquad (1)$$

in terms of the stiffness tensor C_0 of the undamaged material and of the loss of stiffness C_c due to the onset of damage. The variation of the stiffness tensor is selected as an internal variable representing the current state of damage of the material.

Traditionally, the damage varies from zero for the initial state to the critical value D=1 at the failure [23]. It is thus necessary to normalize the components of the damage tensor to their thermodynamically admissible maximum values, so that the elasticity tensor remains a positive definite operator [22]:

$$D_{ii} = 1 - \frac{C_{ii}}{C_{ii}^0} \quad , \; i = 1 \text{ to } 6 \, , \tag{2}$$

$$D_{ij} = \frac{C_{ij}^0 - C_{ij}}{C_{ij}^0 + \text{Sign}(C_{ij}^0 - C_{ij}) \sqrt{C_{ii}^0 (1 - D_{ii}) C_{jj}^0 (1 - D_{jj})}} \quad , i, j = 1,.. , 6, \; i \neq j \, . \tag{3}$$

Variations of the stiffnesses C_{ij} as a function of a tensile stress applied in direction 3 give the change of the damage tensor components D_{ij} using relations (2-3). These changes, Figure 2, are different for each component and show clearly the anisotropy of the damage. As the cracks grow preferentially in the plane perpendicular to the loading direction, the damage D_{33} associated to the stiffness in the tensile axis 3 exhibits an important linear increase, in relation with the observed important loss of stiffness from 123 GPa to 75 GPa. It is worthy of note that this microcracking has also an important effect on shear moduli and particularly on those relative to the planes containing the loading direction (C_{44} and C_{55}). The only non zero components of the damage tensor are therefore D_{33}, D_{44} and D_{55}.

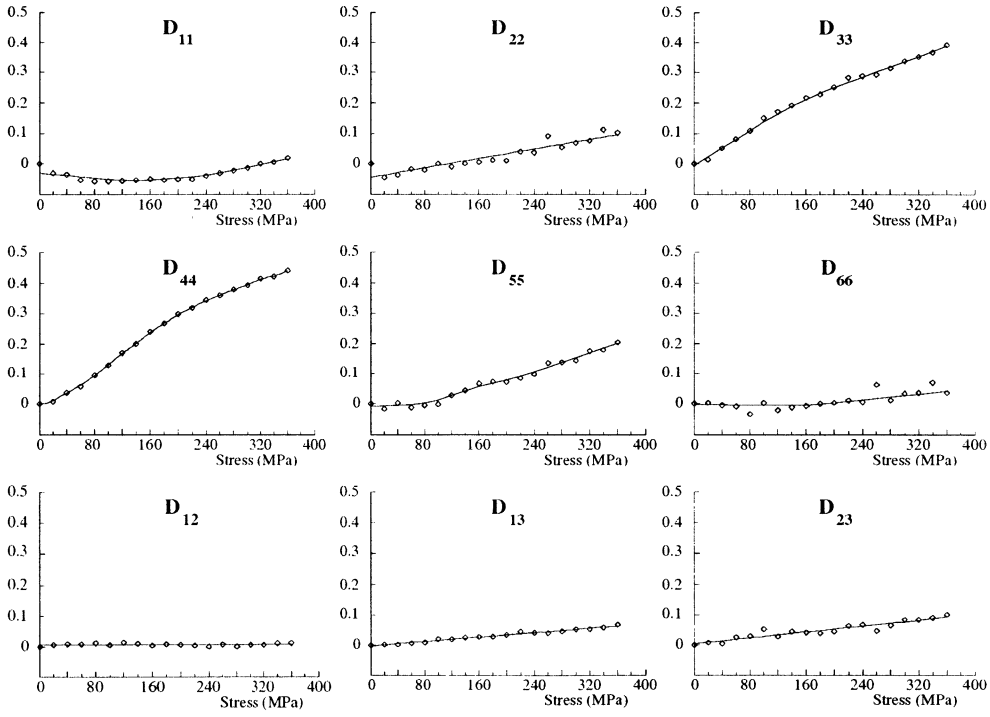

Figure 2. Evolution of the damage tensor coefficients as a function of a tensile stress applied within the fiber direction 3.

FATIGUE RESULTS

The typical fatigue lifetime diagram, Figure 3, is divided in three regions [14]. Region 1 is the "scatter band" of the fiber failure stress. The mechanism operating is fiber failure of catastrophic strain. Region 2 is a sloping band of progressive damage consisting of fiber-bridged matrix cracking where the fiber breakage becomes unstable. The lower limit of this region is where the applied stress is just insufficient to cause instability of the fiber breakage. Region 3 is the region in which the breakage of the crack bridging fibers remains stable. Figure 3 shows the fatigue data reported from [24] for C/SiC composite. The data have been plotted in the fatigue life diagram to facilitate interpretation according to the discussion above. The three domains depending on the maximum fatigue stress applied may be observed. The first domain where the matrix cracking is expected to have been essentially complete in the first cycle and the fibers thus exposed carry the applied load. Failure occurs at random times by a stochastic process of first passage of failure strain of fibers. A second domain above 340 MPa for which progressive fatigue failures were observed after a limited number of cycles (from 10 to 20000). A thirst domain below 340 MPa where no fracture occurred within 10^5 cycles (arbitrarily chosen as fatigue runout). Considering the set of results obtained from the fatigue test program, the fatigue limit may be estimated at 330±10 MPa, which is close to 80% of the average tensile stress to rupture.

Ultrasonic characterization measurements were performed on a sample tested at a maximum fatigue stress of 360 MPa, i.e., over the fatigue limit in order to enhance the various damage mechanisms. As failure occurred after 432 cycles, only 4 characterization cycles were thus recorded, after 1, 10, 100, 200 fatigue cycles, respectively. Damage parameters which have been identified from this test as the most representatives of the fatigue degradation mechanisms are plotted in Figures 4 and 5.

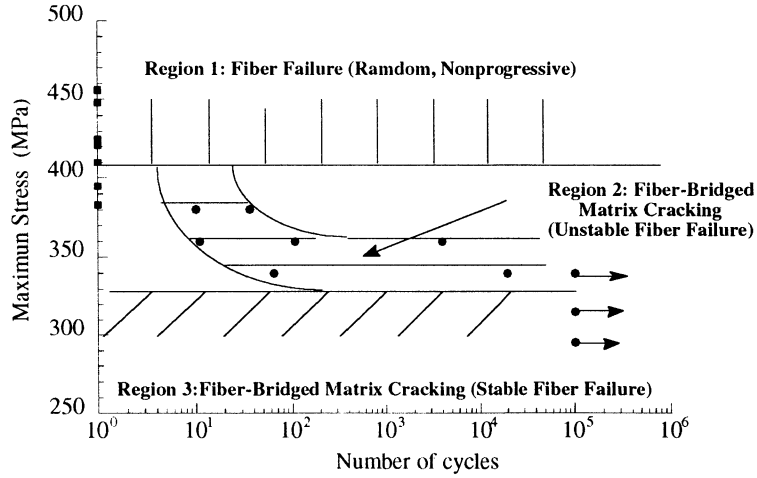

Figure 3. Fatigue lifetime diagram of the C/SiC composite (arrows denote the runout specimens) under tension-tension cycling along fibers.

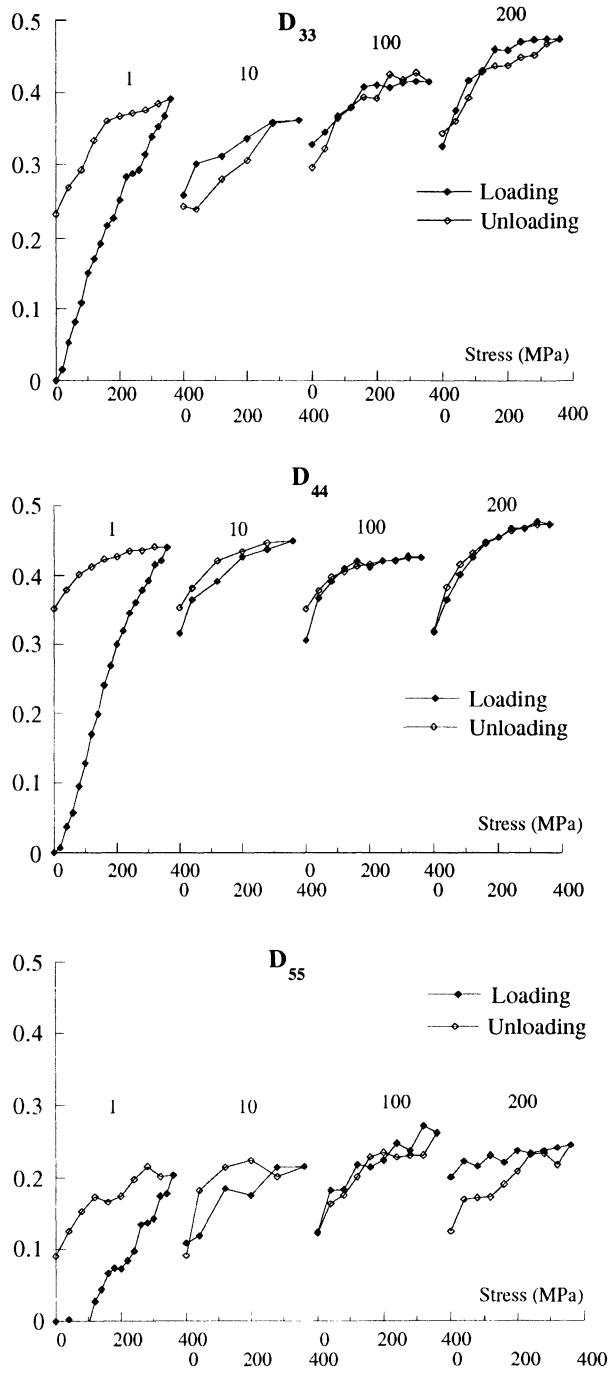

Figure 4. Anisotropic damage coefficients associated to transverse matrix microcracking during fatigue.

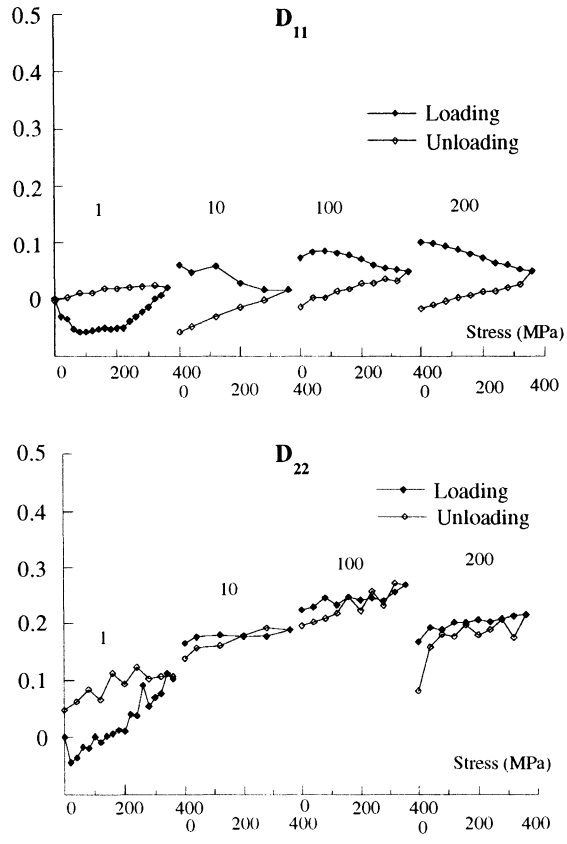

Figure 5. Damage coefficients associated to longitudinal microcracking during fatigue.

Determination of fatigue damage allows tthe determination of three degradation mechanisms. During the first cycle and similar to a tensile test, the three damage coefficients D_{33}, D_{44} and D_{55}, associated to the transverse matrix cracking increased noticeably. Upon the following cycles these three damage coefficients remained stable, Figure 4. They were only affected by the progressive opening-closure of the first cycle created cracks. D_{33}, D_{44} and D_{55} decrease during unloading cycles. The loading cycles progressively reopen these cracks and these damage coefficients reach their previous value.

On the other hand, the damage coefficients D_{11} and D_{22}, associated with longitudinal microcracking, i.e., fiber/matrix debonding, increased noticeably during cycling, Figure 5. The Carbon SiC composite is not initially cohesive. Fatigue cycles increase the fiber/matrix loss of cohesion detected by the damage coefficients D_{22} and D_{11}. When the density of longitudinal cracks becomes large, their interaction with the transverse microcracking induces the composite failure. It is probably the more or less dramatic growing of the loss of cohesion and, so loading transfer to the fibbers that induces the failure of the material loading in fatigue in the high stress domain.

CONCLUSION

The behavior of 2D C/SiC composite, like that of most ceramic matrix composites, is strongly influenced by the nucleation and growth of damage, i.e., matrix microcracks and fiber/matrix partial debonding. The propagation of damage may be measured by the induced changes of the material stiffnesses. Since microcracks have overriding propagation directions, their effect is highly anisotropic and the variations of the whole stiffness tensor must be studied. The use of ultrasonic evaluation allowed the identification of such variations and be proved to be of particular interest in the case of fatigue for which longitudinal damage appeared to be a preponderant mechanism.

ACKNOWLEDGMENTS

Thanks to the Société Européenne de Propulsion for supplying the C/SiC material and for partial funding under contract n°479192.

REFERENCES

1. D. Krajcinovic, Mech. Mater. 8, 117-197 (1989).
2. E.T. Onat and F.A. Leckie, J. Appl. Mech. 55, 1-10 (1988).
3. R. Talreja , Proc. R. Soc. Lond. A399, 195-216 (1985).
4. S.S. Wang, E.S.-M. Chim and H. Suemasu, J. Appl. Mech. 53, 347-353 (1986).
5. P.R. Waynes, J. Issacs and S. Nemat-Nasser, in *Review of Progress in QNDE*, Vol. 8B, eds D. O. Thompson and D. E. (Plenum, New York, 1989), p. 1827-1833.
6. R. El Guerjouma and S. Baste, in *Ultrasonics International 89*, Madrid, July 1989, (Butterworth -Heinemann, 1989), p. 895-900.
7. J. Roux, B. Hosten, B. Castagnède and M. Deschamps, Rev. Phys. Appl. 20, 351-358 (1985).
8. S.Baste and B.Hosten, Rev. Phys. Appl. 25 , 161-168 (1990).
9. B. Audoin and S. Baste, in *ICCM 8*, Honolulu, July 1991, ed. S. W. Tsai and G. S. Springer, (SAMPE, 1991), p. 39-C-1-39-C10.
10. B. Audoin and S. Baste, J. Appl. Mech 61, 309-316 (1994).
11. J. M. Jouin, in *Matériaux composites pour applications à hautes températures*, eds. R. Naslain, J.Lamalle and J.L. Zulian, (AMAC/CODEMAC, Bordeaux, France 1990).
12. D.B. Marshall and A.G. Evans, J. Am. Ceram. Soc. 68 (1985) 225-231.
13. I. M. Daniel and A.Charewicz Eng. fract. Mech. 25, 793-808 (1986).
14. R. Talreja , 1990, in *11 th Ris International Symposium*, eds J.J. Bentzen, J.B. Bilde-Srensen, N. Christansen, A. Horsewell and B. Ralph, (Ris: National Laboratory, 1990), p.145-159.
15. D. Rouby and P. Reynaud, Comp. Sci. and Techno. 48, 109 (1993).
16. L. M. Butkus, L. P. Zawada and G. A. Hartman, in *AeroMat'90*, 21-24 May 1990, Long beach, Ca, (1990).
17. N. Laws, G.J. Dvorak and M. Hejazi, Mech. Mater. 2, 123-137 (1983).
18. Z. G. Wang, C. Laird, Z. Hashin, B. W. Rosen and C. F. Yen, J. Mater. Sci. 26, 4751-4758 (1991).
19. B. A. Auld, *Acoustic fields in solids,* (Wiley-Interscience, New York, 1973), Vol. 1.
20. B. Castagnède, J. T. Jenkins, W. Sachse and S. Baste, J. Appl. Physics 67, 6, 2753-2761 (1990) .
21. B. Hosten, Ultrasonics 30, 6, 365-371 (1992).
22. S. Baste and B. Audoin, Eur. J. Mech. A/Solids 10, 6, 587-606 (1991).
23. J. Lemaitre and J.L. Chaboche, J. Meca. Appl. 2 , 167-189 (1978).
24. G. Camus, R. El Bouazzaoui, S. Baste and F. Abbe, in *World ceramics Congress*, Florence, june 29- july 4 (1994).